J Polym Res (2013) 20:119
DOI 10.1007/s10965-013-0119-3

ORIGINAL PAPER

Synthesis and photovoltaic performance of a fluorene-bithiophene copolymer

Isabel R. Grova · Douglas J. Coutinho
Roberto M. Faria · Leni Akcelrud

Received: 16 October 2012 / Accepted: 4 March 2013 / Published online: 28 March 2013
© Springer Science+Business Media Dordrecht 2013

Abstract We present the synthesis of a copolymer structure, poly(9,9′-*n*-di-hexyl-2,7-fluorene-*alt*-2,5-bithiophene), referred to herein as LaPPS43, and its physico-chemical characterization. Thin films of this polymer mixed with phenyl-C61-butyric acid methyl ester (PCBM) were used as the active layer in photovoltaic devices using the ITO/PEDOT:PSS/LaPPS43:PCBM/Ca/Al bulk heterojunction structure. The devices of different active layer thicknesses were electrically studied using J-V curves and the Photo-Celiv technique. The obtained results show that LaPPS43 combined with PCBM is a promising system for photovoltaic devices. Device performance is discussed in terms of the mean drift distance x for charge carriers. Photophysical data showed that the excitonic species are all localized in the aggregated forms. The mechanism of exciton formation and dissociation is also discussed.

Keywords Synthesis · Polythiophene derivatives · Photovoltaic properties · Solar cells

I. R. Grova · L. Akcelrud (✉)
Paulo Scarpa Polymer Laboratory (LaPPS),
Federal University of Parana, CP 19081,
CEP 81531-990, Curitiba, Paraná, Brazil
e-mail: leni@leniak.net

I. R. Grova
e-mail: isabelgrova@yahoo.com.br

I. R. Grova · L. Akcelrud
Integrated Graduate Program in Engineering (PIPE),
Federal University of Parana, CP 19011,
CEP 81531-990, Curitiba, Paraná, Brazil

D. J. Coutinho · R. M. Faria
Group of Polymers "Bernhard Gross" – Physics Institute of São Carlos, Institute of Physics, São Paulo University (USP), P.O. Box 369, CEP 13084-971, São Carlos, São Paulo, Brazil

Introduction

Conjugated polymers are now definitively considered active materials for electronic and optoelectronic devices, such as electroluminescent devices, transistors and photovoltaics [1–3]. They have a combination of good semiconducting properties with good thermal and mechanical properties that allow for the production of efficient devices at low cost. Among these devices, organic photovoltaics are one of the most promising; several new polymeric structures have been specially synthesized for this application. Recently, the combination of fluorene and thiophene groups to form a single repeating unity has produced donor-copolymers, which when combined with acceptor species, yield high performing solar cells. The incorporation of the fluorine unit has been widely used because it has good open circuit voltage (V_{oc}) values due to its relatively low HOMO (*Highest Occupied Molecular Orbital*) level. For charge generation, the insertion of an acceptor species is needed, such as phenyl-C61-butyric acid methyl ester (PCBM) that has been employed in the majority of the published data [4]. Copolymerization, on the other hand, is a classical polymer science tool for incorporating the properties of parent homopolymers into a single material, and in the present application, for inserting electron withdrawing units into a fluorene polymer backbone to produce low gap materials [5]. The overall efficiency of organic solar cells is dictated by four main processes: absorption (the creation of bound electron–hole pairs known as excitons), charge generation (the dissociation of excitons into free carriers), recombination and/or collection as carriers to their respective electrodes. The close proximity of the donor and acceptor components is a major advantage of bulk heterojunction devices (BHJ). Compared to the bilayer configuration, higher overall results were obtained with the BHJ architecture [6].

Polythiophene and its derivatives have been shown to possess better charge carrier mobilities as hole transporters than other conjugated materials. The combination of

fluorene and thiophene units in various copolymers with different molecular configurations have been explored in solar cell studies [7]. Recently, the best power conversion efficiency (PCE) achieved with polymer solar cells (PSCs) with a bulk heterojunction (BHJ) configuration was above 5 % [8]. With the application of macromolecular engineering techniques, new fullerene derivatives and improvements in device architecture, it has been predicted that 10 % efficiency can be achieved in a few years [9].

This paper deals with the copolymer poly(9,9′-*n*-di-hexyl-2,7-fluorene-*alt*-2,5-bithiophene) (LaPPS43). Although the structure has been already reported, the results correlating chemical structure and device characteristics are scarce; the present work aims to extend the knowledge of its properties in order to better explore the full potential of this polymer. The most promising results have been obtained in photovoltaic devices using hole transport measurements with the time-of-flight (TOF) technique. The simple solar cells prepared by blending the polymer with fullerene; presented a PCE of 2.4 % with an open-circuit voltage of approximately 0.9 V and a fill factor of approximately 50 % [9]. PCE values of 2.46 % in tandem cells have also been reported [10], while 3 % was attained using the "solvent annealing" procedure [11]. In a recent publication [12], we reported a PCE of 2.8 % in a bilayer configuration. Here a bulk structure was built to probe the role of the device parameters in its behavior, in particular the influence of the active layer thickness The synthesis, the physico-chemical characterization of the material as thin films are reported along with the first results of photovoltaic activity for ITO/PEDOT:PSS/LaPPS43:PCBM/Ca/Al BHJ structures using different thicknesses of the active layer. Studies of the transport properties were also conducted using the Photo-Celiv technique. The photophysical properties were described as well.

Materials and methods

Synthesis of poly(9,9′-n-di-hexyl-2,7-fluorene-alt-2,5-bithiophene)

The electronic polymer LaPPS43 was synthesized by the Suzuki Cross Coupling Condensation method [13, 14], as shown in Fig. 1. For this synthesis, we used commercially available materials. Tetrakis-(triphenylphosphin)-palladium (0) ($Pd(PPh_3)_4$), 5,5′dibromo-2,2′-bithiophene, 9,9′-dihexylfluorene-2,7-diboronic acid, and 2-bromobenzene were purchased from Aldrich. Magnesium sulfate ($MgSO_4$) and silica gel for chromatography (0.035–0.070 mm (60 Å)) were purchased from Acros. A degassed mixture of toluene (40 mL) and aqueous (2 M) potassium carbonate (11.7 mL) was added to a mixture of 5,5′dibromo-2,2′-bithiophene (500 mg, 1.54 mmol), 9,9′-dihexylfluorene-2,7-diboronic acid (683 mg, 1.62 mmol) and tetrakis(triphenylphosphine) palladium(0) (37 mg). The final product was vigorously stirred at 90 °C for 5 days under a nitrogen environment. At the end of the polymerization, the terminal boronic acid group was end-capped by adding excess 2-bromobenzene (0.218 mL) in a toluene solution (5 % of the total volume). The emulsion was vigorously stirred at 90 °C for 12 h. The reaction mixture was then cooled to room temperature and slowly added to a stirred mixture of methanol, acetone, and HCl (1 M). The polymer was collected by filtration and then purified by chromatography (silica gel, $CHCl_3$), followed by Soxhlet extraction in methanol, resulting in an yield of 89.5 %.

^{1}H NMR spectra were recorded on a Brücker AC 400 MHz spectrometer using $CDCl_3$ solvent. NMR ^{1}H (400 MHz, $CDCl_3$, δ em ppm): 0.76 (brm,10H), 1.09 (brm, 12H), 2.05 (brm, 4H), 7.15–7.35 (brm, 4H), 7.51–7.60 (brm, 6H). Elemental analyses were performed on a Perkin-Elmer CHNS 2400 elemental analyzer. Anal. Calcd for $C_{33}H_{36}S_2$: C, 79.8; H, 7.25; S, 12.9. Found: C,76.5; H, 7.25;S,11.03.

Gel permeation chromatography (GPC) analyses were run on a Waters 1515 separation module using polystyrene as the standard and tetrahydrofuran (THF) as the eluent. The transition temperatures of films were determined by differential scanning calorimetry on a Netzsch DSC 204 F1 with N_2 atmosphere; heating and cooling rates of 10 °C/min and a flow rate of 15 mL/min were used. Thermogravimetric analyses (TGA) were performed on a Netzsch TG 209 thermogravimetric analyzer under nitrogen, with a heating rate of 20 K/min. UV-visible absorption spectra were recorded in chloroform solutions and in films on a Shimadzu NIR3101 spectrophotometer. The fluorescence

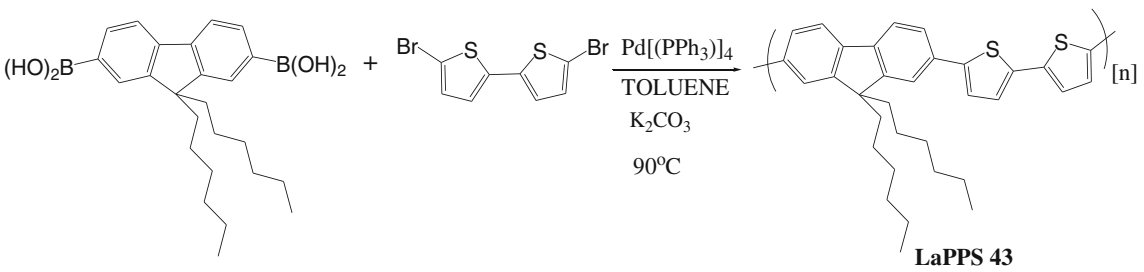

Fig. 1 Chemical route to Poly(9,9′-n-di-hexyl-2,7-fluorene-*alt*-2,5-bithiophene) - LaPPS 43

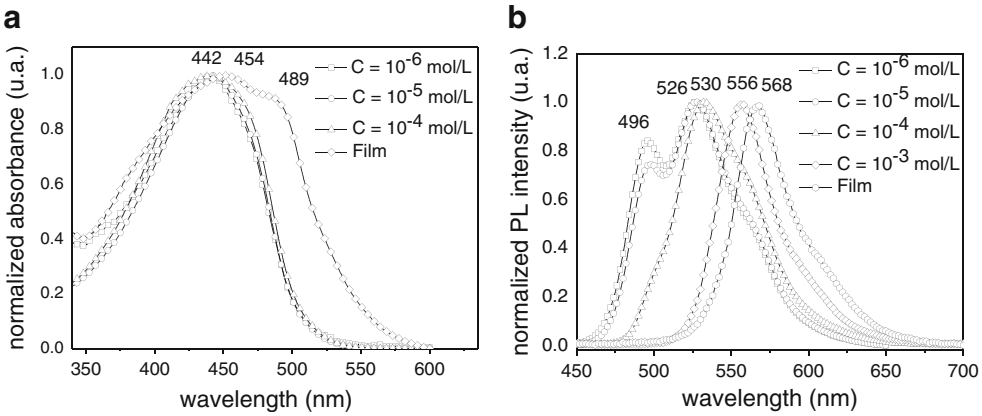

Fig. 2 **a**) UV-visible absorption spectra and **b**) emission spectra of chloroform solutions with different concentrations and the thin film (coated onto a fused quartz plate) of LaPPS 43

(PL) spectra were obtained on a Shimadzu RF5301PC spectrophotometer.

Device preparation

Thin films of the LaPPS43:PCBM composite (50 to 170 nm thick) were prepared by spin casting on an appropriate substrate under a nitrogen environment. Organic photovoltaic devices (OPVs) were then built using these films. A solution of poly(9,9′-n-di-hexyl-2,7-fluorene-*alt*-2,5-bithiophene) and phenyl-C61-butyric acid methyl ester (PCBM) was prepared with chloroform as a solvent (1:3 by weight). The substrate was composed of commercial ITO glass substrates (Delta Technologies®) covered by a thin layer of PEDOT:PSS (Baytron®). The used ITO had a sheet resistivity of 8 to 12 Ohms/square and a thickness of approximately 100 nm with a roughness of 4 nm. These data, provided by the company, were confirmed in our laboratories using a Dektak 150 perfilometer (Veeco) and a Nonoscope III AFM (Digital). Anodes were formed by removing parts of the ITO using a corrosive HCl solution (1 M) and then washed with an ethanolamine solution made with MILLI-Q water. The ITO was then immersed in an ethanolamine solution at 80 °C for 20 min and then in isopropyl alcohol at 60 °C for another 20 min then dried in a nitrogen flux. Finally, the ITO was exposed to UV light to improve its wettability in order to facilitate the deposition of the PEDOT:PSS layer by spin casting. Finally, the cathode bilayer of calcium (30 nm) and aluminum (100 nm) was formed by vacuum evaporation. The final devices had an area of 10 mm^2.

Electrical and optical characterization

J-V measurements of the photovoltaic cells were carried out using a 2400 Keithley electrometer under vacuum. To characterize the solar cell we used an AM 1.5 solar spectral irradiance setup. A similar system with a monochromator was used to obtain the IPCE of the cells. The Photo-Celiv technique was used to measure the carrier mobility. This technique uses a linear voltage ramp (LVR) triggered after a delay time τ_{delay} (~1 μs) after the incidence of a short laser pulse. The wavelength of the laser is such that the absorption coefficient is very low, thus generating a uniform distribution of photocarriers. The transient current Δj (difference between the two recorded currents, with and without illumination) is directly related to the amount of photocarriers and is used in the calculation of the carrier mobility by Eq. (1) [15].

$$\mu = \frac{2d^2}{3A\tau_{\max}^2\left(1 + 0.36\frac{\Delta j}{j(0)}\right)} \quad (1)$$

where d is the film thickness, A is the voltage rate of LVR, τ_{max} is the time of the peak Δj, and $j(0)$ is the displacement current in a sample without photocarriers.

Results and discussion

Synthesis and characterization

The polymerization reaction of LaPPS43, depicted in Fig. 1, was based on the palladium catalyzed Suzuki cross coupling reaction. The Suzuki coupling methodology is not sensitive to the presence of water but is sensitive to oxygen and light. The

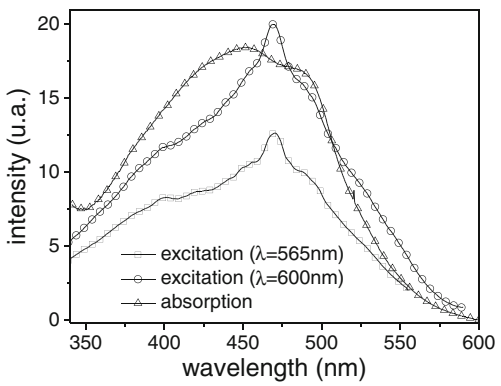

Fig. 3 Excitation and UV-visible absorption spectra in the film form (coated onto a fused quartz plate) of LaPPS 43

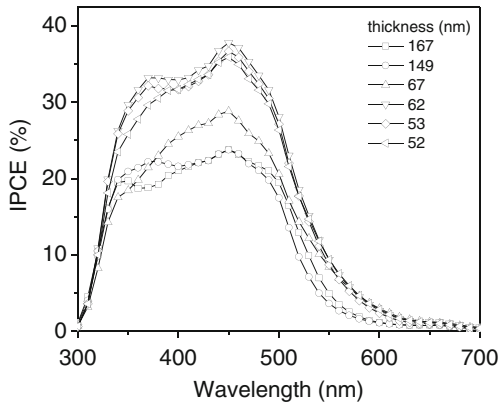

Fig. 4 The variation of the external quantum efficiency (IPCE) of the cells with thickness

chemical structure of the polymer was confirmed by ^{1}H-NMR spectra; the chemical shifts were recorded in parts per million (ppm) and referenced to TMS (δ=0 ppm for ^{1}H-NMR) The typical chemical shifts of fluorene (7.15–7.35 ppm) and bithiophene (7.51–7.60 ppm) were clearly defined. The polymer was then dissolved in common organic solvents, such as chloroform, THF and toluene, resulting in a dark orange color. The average molecular weight, determined by gel permeation chromatography (GPC) using polystyrene as the standard, was found to be 6,500 and 15,400, for Mn and Mw, respectively, with a polydispersity index of 2.37.

Thermal stability

The thermal stability of LaPPS43, under a nitrogen atmosphere, was determined by TGA, while the conformational or phase transitions were analyzed by differential scanning calorimetry (DSC). The polymer showed excellent thermal stability with a decomposition temperature of 300 °C (onset of weight loss) and a glass transition temperature of 97 °C. The high decomposition and glass transition temperatures of LaPPS43

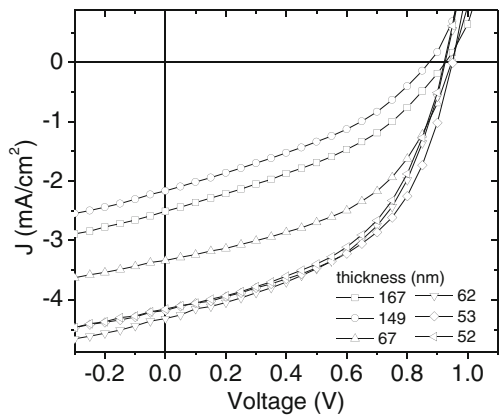

Fig. 5 *J-V* curve for solar cells of ITO/PEDOT:PSS/LaPPS43:PCBM(1:3)/Ca/Al under AM 1.5 G illumination and an irradiation intensity of 100 mW/cm^2

Table 1 Photovoltaic characteristics and thicknesses of the active layer

Thickness (nm)	J_{sc} (mA/cm^2)	V_{oc}(V)	FF (%)	η (%)
167	2.50	0.93	38	0.88
149	2.16	0.87	36	0.68
67	3.33	0.95	48	1.51
62	4.31	0.93	48	1.92
53	4.17	0.95	50	1.98
52	4.15	0.92	49	1.87

are adequate for applications in optoelectronic devices or other devices that operate at room temperature [9, 10, 16].

Optical properties

Figure 2 shows the UV-visible absorption and emission spectra of LaPPS43 in film and in solutions (different concentrations). All the absorption curves exhibited a maximum at 442 nm. The absorption spectra obtained in solution did not change with concentration, while the thin film form presented an additional band at approximately 490 nm. The emission spectra of the solutions show two main noteworthy features. Firstly, the more diluted solutions displayed two characteristic vibronic bands at 496 nm and 526 nm [17], and a shoulder was also recorded at around 565 nm. Secondly, a strong redshift of the whole spectrum took place as the concentration increased. Additionally, the first vibronic band, which has the lowest wavelength, visibly weakened as the concentration increased. This behavior is typical of the aggregate emission [18–20]. The origin of the absorption at 490 nm could be ascribed to the presence of preformed dimmers or even higher forms of association in the electronic ground state. The emission of the isolated fluorene moiety (at approximately 413 nm [21]) was not detected. The excitation spectra monitored at 565 nm and 600 nm, shown in Fig. 3, supports the assumption that only the preformed ground state dimmers are the emitting species;

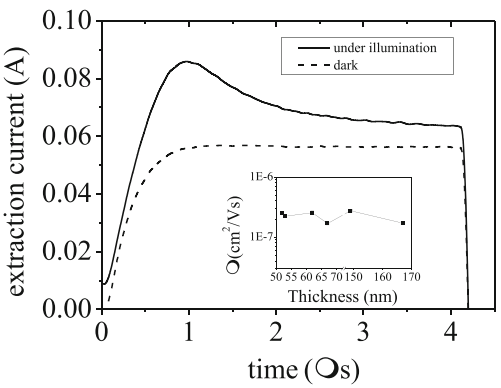

Fig. 6 Extraction current obtained from the photo-celiv technique

that is, the excitonic species are all localized in the aggregated forms. This does not mean that excitons on the single chromophores are not formed, but rather that the energy transfer from the aggregates is a faster process than single molecule decay. The broadness of the film spectra reflects the presence of a large number of conformational states which were frozen during solvent evaporation. The absorption onset obtained from the thin films was used to estimate the band gap (Eg) of LaPPS43, which was 2.20 eV. Two possible pathways for exciton transfer/dissociation should be considered, in terms of time decay and morphology. The aggregated sites can act as traps for the single chromophore excitons when there is no fullerene in the neighborhood, and at the same time the dissociation and transfer from the aggregates to the C60 cannot be disregarded.

Photovoltaic properties

Figure 4 shows the internal quantum efficiency (IPCE) obtained directly from the ITO/PEDOT:PSS/LaPPS43:PCBM(1:3)/Ca/Al structures with different thicknesses of the LaPPS43:PCBM composite, the active layer of the device. The IPCE provides the number of charge carriers collected per absorbed photon by the active layer of the solar cell. It is well-known that ITO and PEDOT:PSS show a weak absorption in the visible region and that the photon-to-charge conversions are negligible in such layers [22]. The IPCE shows that the LaPPS43:PCBM composite is a promising mixture for photovoltaic applications and the best performances were observed for layers in between 50 and 60 nm. This is in agreement with the calculated absorption for a similar polymeric system using a transfer matrix approach [23], where the charge generation rate profile showed a maximum at approximately 65 nm.

The IPCE was in agreement with the *J-V* photovoltaic response of these devices, as shown in Fig. 5. The best *J-V* curves, under AM 1.5 G illumination and an irradiation intensity of 100 mW/cm^2, were obtained with the thinner active layers (below 65 nm). The results of devices having similar active layer thicknesses (52 and 53 nm) show the reproducibility of these organic photovoltaic devices. The characteristic values of each OPV device are shown in Table 1. Short-circuit current, fill-factor and efficiency increases as the thickness decreases; however, the open-circuit voltage seems to be independent of thickness.

The good performance, as exhibited by the number of charge carriers generated per absorbed photon (IPCE curves), was not confirmed by the numbers shown in Table 1, where the best efficiency was 2 %. The electrical properties of the devices were investigated using the Photo-Celiv technique [24, 25]. These measurements were carried out on the complete ITO/PEDOT:PSS/LaPPS43:PCBM(1:3)/Ca/Al devices with the different thicknesses of the active layers (52, 53,62, 67, 149, and 167 nm). A typical Photo-Celiv response is shown in Fig. 6; the mobilities of charge carriers, calculated from Eq. 1, are independent of the thickness (inset in Fig. 6). The obtained mobilities showed an average value of 2×10^{-7} cm^2/V·s. This low value is a possible explanation for the relatively low performance of these structures as photovoltaic devices.

Conclusions

This paper presents the synthesis and characterization of a conjugated polymeric structure that can be used as an active material in solar cells. It is a copolymer based on a fluorene derivative and two thiophene rings: poly(9,9′-n-di-hexyl-2,7-fluorene-*alt*-2,5-bithiophene). It exhibited good thermal stability and adequate optical and photon-to-charge carrier conversion properties. However, it is necessary to improve its electrical properties, mainly its electrical mobility, the first step of which is to improve the film morphology. The charge generation rate is one of the most important factors determining device performance. However, the charge migration dynamics is also crucial for good devices. The mean drift distance x of the carrier in a given electric field ($\mu\tau E$) is an important parameter that is directly related to the electronic properties of the polymer and the morphology of the thin films. τ is the trapping time for the charge carriers. This parameter can explain why the performances of the thin layers (52 and 67 nm) are much better than those of the thick layers (149 and 167 nm) (Fig. 5). If x is close to the active layer thickness and the electric field is approximately 10^5V/cm, the trapping time for the carriers would be at approximately 100 μs, which is compatible with values found for conjugated polymers [26, 27].

Acknowledgments The authors are indebted to CNPQ, INEO, PIPE, and UFPR for their financial support.

References

1. Shirota Y (2000) J Mat Chem 10:1–25
2. Laquai F, Park YS, Kim JJ, Basche T (2009) Macrom Rap Comm 14:1203
3. Bianchi RF, Onmori RK, Faria RM (2005) J Polym Sci: Part B: Polym Phys 43:74–78
4. Brabec CJ, Cravino A, Meissner D, Sariciftci NS, Fromherz T, Rispens MT, Sanchez L, Hummelen JC (2001) Adv Funct Mater 11:374
5. Piyakulawat P, Keawprajak A, Jiramitmongkon K, Hanusch M, Wlosnewski J, Asawapirom U (2011) Solar Energy Mater Solar Cells 95:2167–2172
6. Homa B, Andersson M, Inganäs O (2009) Org Electron 10:501–505

7. Zhao B, Liu D, Peng L, Li H, Shen P, Xiang N, Liu Y, Tan S (2009) Eur Polym J 45:2079–2086
8. Du C, Li C, Li W, Chen X, Bo Z, Veit C, Ma Z, Wuerfel U, Zhu H, Hu W, Zhang F (2011) Macromolecules 44:7617–7624
9. Tang W, Chellappan V, Liu M, Chen Z-K, Ke L (2009) Appl Mater Interfaces 1:1467–1473
10. Zhao D, Tang W, Ke L, Tan ST, Sun XW (2010) Appl Mater Interfaces 2:829–837
11. Schulz GL, Chen X, Holdcroft S (2009) Appl Phys Lett 94:023302
12. Macedo AG, Marchiori CFN, Grova IR, Akcelrud L, Koehler M, Roman LS (2011) Appl Phys Lett 98:253501
13. Xia C, Advincula RC (2001) Macromolecules 34:5854–5859
14. Zeng L, Yan F, Wei SK-H, Culligan SW, Chen SH (2009) Adv Funct Mater 19:1978–1986
15. Juska G, Arlauskas K, Viliunas M, Geneviczius K (2000) Phys Rev B 62:235
16. Tang W, Ke L, Tan L, Lin T, Kietzke T, Chen Z-K (2007) Macromolecules 40:6164–6171
17. Scherf U, List EJW (2002) Adv Mater 14:477
18. Giro R, Davila LYA, Machado, Caldas MJ, Akcelrud L (2008) Int J Quantum Chem 109:885–892
19. Tozoni JR, Guimarães FEG, Atvars TDZ, Nowacki B, Akcelrud L, Bonagamba TJ (2009) Eur Polym J 45:2467–2477
20. Rodrigues PC, Grova I, Coutinho DJ, Domingues RA, Oh HS, Seo J, Faria RM, Atvars TDZ, Prasad PN, Akcelrud L (2012) J Polym Res 19:9828
21. Klaerner G, Miller RD (1998) Macromolecules 31:2007–2009
22. Häusermann R, Knapp E, Moos M, Reinke NA, Flatz T, Ruhstaller B (2009) J Appl Phys 106:104507
23. Hwang I, McNeill CR, Greenham NC (2009) J Appl Phys 106:094506
24. Mozer AJ, Sariciftci N, Lutsen L, Vanderzande D, Osterbacka R, Westerling M, Juska G (2005) Appl Phys Lett 86:112104
25. Faria GC, Faria RM, de Azevedo ER, Seggern HV (2011) J Phys Chem C 115:25479–25483
26. McNeilla CR, Greenham NC (2008) Appl Phys Lett 93:203310
27. Pensack RD, Banyas KM, Asbury JB (2010) J Phys Chem C 114:5344–5350